Published in final edited form as:
J Alzheimers Dis. 2009 December ; 18(4): 885–896. doi:10.3233/JAD-2009-1196.

Galanin Fiber Hyperinnervation Preserves Neuroprotective Gene Expression in Cholinergic Basal Forebrain Neurons in Alzheimer's Disease

Scott E. Counts[a], **Bin He**[a], **Shaoli Che**[b,c], **Stephen D. Ginsberg**[b,c,d], and **Elliott J. Mufson**[a,*]

[a]Department of Neurological Sciences, Rush University Medical Center, Chicago, IL, USA

[b]Center for Dementia Research, Nathan Kline Institute, New York University Langone Medical Center, Orangeburg, NY, USA

[c]Department of Psychiatry, New York University School of Medicine, Orangeburg, NY, USA

[d]Department of Physiology and Neuroscience, New York University School of Medicine, Orangeburg, NY, USA

Abstract

Fibers containing galanin (GAL) hyperinnervate cholinergic basal forebrain (CBF) nucleus basalis neurons in late stage Alzheimer's disease (AD), yet the molecular consequences of this phenomenon are unknown. To determine whether GAL alters the expression of genes critical to CBF cell survival in AD, single cell microarray analysis was used to determine mRNA levels within nucleus basalis neurons lacking GAL innervation from subjects who died with a clinical diagnosis of no cognitive impairment (NCI) compared to nucleus basalis neurons from AD cases either lacking GAL hyperinnervation (AD/GAL−) or those displaying prominent GAL hyperinnervation (AD/GAL+). Levels of mRNAs encoding putatively neuroprotective proteins such as the GluR2 Ca^{2+}-impermeable glutamate receptor subunit, superoxide dismutase 2, and the GLUT2 glucose transporter were significantly decreased in AD/GAL− nucleus basalis neurons compared to NCI and AD/GAL+ neurons. By contrast, mRNAs encoding calpain catalytic and regulatory subunits, which may contribute to cell death in AD, were increased in AD/GAL−compared to NCI and AD/GAL+ neurons. Hence, GAL fiber hyperinnervation appears to preserve the expression of genes subserving multiple neuroprotective pathways suggesting that GAL overexpression regulates CBF neuron survival in AD.

Keywords

Alzheimer's disease; antioxidant; calcium; calpain; cholinergic basal forebrain; galanin; glucose transporter; glutamate receptor; nucleus basalis; ubiquitin

INTRODUCTION

The neuropeptide galanin (GAL) regulates the activity of cholinergic basal forebrain (CBF) neurons [1–5]. These cells project to the neocortex and hippocampus [6] where they modulate

*Corresponding author: Elliott J. Mufson, PhD, Alla and Solomon Jesmer Chair in Aging, Professor of Neurological Sciences, Rush University Medical Center, 1735 West Harrison Street Suite 300, Chicago, IL 60612, USA. Tel.: +1 312 563 3569; Fax: +1 312 563 3571; emufson@rush.edu.

attentional processes and memory function [7–9]. Significantly, CBF cortical projection neurons of the nucleus basalis (NB) undergo selective degeneration during the later stages of Alzheimer's disease (AD) [10,11], which correlates with clinical severity and disease duration [12,13]. Several groups have made the striking observation that CBF neurodegeneration in late stage AD is accompanied by the enlargement and hyperinnervationof GAL-containing fibers onto surviving cholinergic NB neurons [14–16]. Furthermore, GAL protein concentration increases two-fold [17] and [^{125}I]-GAL binding increases three-fold [18] within the NB in late stage AD compared to age-matched controls. Whether this GAL plasticity response in AD is deleterious or neuro-protective for surviving cholinergic NB neurons is unknown [19]. To approach this problem from a molecular profiling standpoint, we combined single cell RNA amplification and custom-designed microarray analysis to quantify the levels of multiple functional classes of mRNAs within individual cholinergic NB neurons microaspirated from postmortem tissue of elderly subjects with no cognitive impairment (NCI) or late stage AD. Gene expression profiles were compared among individual cholinergic NB neurons lacking GAL innervation from NCI and AD (AD/GAL−) brains compared to NB neurons hyperinnervated by GAL (AD/GAL+) from the same AD cases.

MATERIALS AND METHODS

Subjects

Brain tissue from NCI (n = 6) and late stage AD (n = 6) cases matched for age and postmortem interval (Table 1) were obtained from the Rush AD Center Brain Bank. NCI subjects exhibited no age-adjusted impairmentin cognition basedonabatteryof neuropsy-chological tests and neurological examination [20–23]. The clinical diagnosis of AD was made following a standardized evaluation utilizing NINCDS/ADRDA criteria [24]. The cognitive status of the NCI and AD groups was estimated using the Mini Mental State Exam (Table 1) [25].

Pathological evaluation and tissue preparation

Brains were removed at autopsy and processed as previously reported [21–23,26]. Brains were cut into 1-cm thick slabs on a Plexiglas brain cutting apparatus. Slabs from one hemisphere were immersion-fixed for 48 hr in 4% paraformaldehyde and cryoprotected [23]. Slabs from the opposite hemisphere were snap-frozen inliquid nitrogen. Aneuropathologist conducted a gross examination of brain neuropathology and cases were excluded if they exhibited significant non-AD types of pathologic conditions (e.g., brain tumors, encephalitis, large strokes, multiple lacunar infarctions). A complete microscopic neuropathological analysis was performed on 8 μm thick paraffin-embedded sections with special attention to lesions that might contribute to dementia, including brainstem and cortical Lewy bodies as well as strokes. A pathological diagnosis was made for each case based on Consortium to Establish a Registry for Alzheimer's Disease (CERAD) criteria [27].

Immuohistochemistry

All immunohistochemical procedures were performed using RNase free conditions as previously reported [28–30]. Paraformaldehyde-fixed tissue was cut on a freezing sliding microtome into 40 μm thick sections through the anterior NB subfield at the level of the decussation of the anterior commissure [6]. The anterior NB subfield shows the greatest degree of GAL hyperinnervation within the CBF in late stage AD [14–16]. Sample sections were confirmed to have abundant RNA species by acridine orange histofluorescence [28,30,31]. To visualize the putative cellular appositions between GAL-immunoreactive (-ir) profiles and cholinergic NB neurons, sections were processed according to a previously described double label procedure that results in an easily identifiable two-colored immunohistochemical profile [16,28,32]. Tissue sections were washed several times in Tris-buffered saline (TBS, pH 7.4) and incubated for 20 minutes in TBS/0.1 M sodium periodate to eliminate endogenous

peroxidase activity. Sections were blocked for 30 minutes in TBS/0.25% Triton X-100 (TX) with 10% normal goat serum (NGS) and then incubated overnight at ambient room temperature (RT) with rabbit polyclonal GAL antiserum (1:15,000; Peninsula Labs, Belmont, CA) in TBS/TX and 1% NGS. Following primary antibody incubation, sections were rinsed and incubated for one hour at RT with biotinylated goat anti-rabbit IgG (1:200; Vector Laboratories, Burlingame, CA) followed by a one-hour incubation with avidin-biotin complex reagent (ABC, 1:500; Vector Laboratories). The sections were then reacted with 0.05% 3,3'-diaminobenzidine (DAB), 0.005% H_2O_2, and 2.5% nickel II sulfate in acetate-imidazole buffer to yield a dark blue-black reaction product labeling GAL positive profiles (Fig. 1). Cholinergic neurons were subsequently labeled using an antibody to the low affinity nerve growth factor receptor $p75^{NTR}$, which is an excellent marker for CBF neurons [33]. For this procedure the sections were blocked in TBS/TX/3% normal horse serum and incubated overnight at RT with a mouse monoclonal $p75^{NTR}$ antibody (1:40,000; Neomarkers, Fremont, CA). The sections were then rinsed, sequentially incubated for one hour at RT with biotinylated horse anti-mouse IgG (1:200, Vector Labs) and ABC (1:500), and then reacted with a non-metallic chromogen solution containing 0.05% DAB and 0.005% hydrogen peroxide to yield a brown reaction product labeling CBF neurons and fibers (Fig. 1). Finally, tissue was mounted onto gelatin-coated slides, dried overnight, and then storedat 4°C without cover slipping in RNase-free phosphate buffer (pH 7.4).

Immunohistochemistry controls

The specificity of the mouse monoclonal $p75^{NTR}$ antibody is well-established [21,33,34]. To gauge the specificity of the GAL antiserum, tissue sections were processed as described above except that the primary antibody was either omitted or was substituted for an irrelevant IgG matched for protein concentration. In addition, we preadsorbed the GAL antiserum 24 hours prior to tissue incubation by adding 1 mM or 10 mM of the synthetic GAL peptide (Peninsula Labs) [28,32]. These sections showed no positive tissue immunoreactivity. It should be noted that these controls are not absolute and the potential for antibody cross-reactivity with structurally related proteins could not be excluded. Thus, GAL immunostaining in this report refers to GAL-"like" immunoreactivity.

Operational characteristics of GAL hyperinnervated NB neurons

It is extremely difficult toquantify alterations in GAL containing axonal terminals and fibers in absolute numbers in the human brain [14–16]. Therefore, the degree of hyperinnervationof GAL-ir profiles onto cholinergic NB neurons was evaluated using a semi-quantitative score indicating the degree of innervation [1 = none to very little (Fig. 1A), 2 = moderate (Fig. 1B), and 3 = dense innervation (Fig. 1C, D)] [28,32,35]. Scores were based on an evaluation of both the density and thickness of GAL fibers impinging upon the NB neuron of interest. For this study, NCI and AD/GAL− NB neurons met the criteria for a score of 1, whereas AD/GAL+ NB neurons were scored with a 3 [35].

Single cell gene expression analysis

Individual $p75^{NTR}$-ir cholinergic NB neurons lacking significant GAL innervation from NCI cases (n = 32) and AD cases (AD/GAL−; n = 30; score = 1) and GAL-hyperinnervated NB neurons from AD cases (AD/GAL+; n = 33; score = 3) were aspirated from dual-labeled tissue using a micromanipulator and microcontrolled vacuum source (Eppendorf, Westbury, NY) attached to a Nikon (Melville, NY) inverted microscope. The amplification of RNA from individual NB neurons was performed using terminal continuation (TC) RNA amplification methodology [36–38]. Each neuron was extracted individually in 250 μl of Trizol reagent (Invitrogen, Carlsbad, CA). RNAs were reverse transcribed in the presence of the poly d(T) primer (10 ng/μl) and TC primer (10 ng/μl) in 1X first strand buffer (Invitrogen),1 mM dNTPs,

5 mM DTT, 20 U of RNase inhibitor and 5 U reverse transcriptase (Superscript III; Invitrogen). The synthesized single stranded cDNAs were convertedinto double stranded cDNAs by adding into the reverse transcription reaction the following: 10 mM Tris (pH 8.3), 50 mM KCl, 1.5 mM $MgCl_2$, 0.5 U RNase H (Invitrogen), and 5 U *Taq* polymerase (Applied Biosystems, Foster City, CA) in a total volume of 100μl. Samples were placedin athermal cycler and second strand synthesis proceeded as follows: RNase H digestion step 37°C, 10 min.; denaturation step 95° C, 3 min., annealing step 50°C, 3 min.; elongation step 75°C, 30 min. The reaction was terminated with 5 M ammonium acetate. The samples were extracted in phenol:chloroform:isoamyl alcohol (25:24:1) and ethanol precipitated with 5 μg of linear acrylamide as a carrier. The solution was centrifuged at 18,000 × *g* and the pellet washed once with 95% ethanol and air-dried. The cDNAs were resuspendedin 20 μl of RNase free H_2O and drop dialyzed on 0.025 μm filter membranes (Millipore, Billerica, MA) against 50 ml of 18.2 mega Ohm RNase-free H_2O for 2 hours. The sample was collected off the dialysis membrane and hybridization probes were synthesized by *in vitro* transcription using ^{33}P incorporation in 40 mM Tris (pH 7.5), 7 mM $MgCl_2$, 10 mM NaCl, 2 mM spermidine, 5 mM of DTT, 0.5 mM of ATP, GTP, and CTP, 10 μM of cold UTP, 20 U of RNase inhibitor, T7 RNA polymerase (1000 U, Epicentre, Madison, WI), and 20 μCi of ^{33}P-UTP (GE-Healthcare, Piscataway, NJ). The reaction was performed at 37°C for 6 hours. Radiolabeled TC RNA probes were hybridized to custom-designed cD-NA arrays without further purification. Two to three hybridization probes were synthesized from the cDNA of each NB neuron and hybridized to the custom arrays in independent experiments.

Custom-designed cDNA array platforms

Array platforms consisted of 1 μg of linearized cDNA purified from plasmid preparations adhered to high-density nitrocellulose (Hybond XL, GE-Amersham) [30,37,39]. Each cDNA and/or expressed sequence-tagged cDNA (EST) was verified by sequence analysis and restriction digestion. cDNA clones and ESTs from mouse, rat, and human were employed. Approximately 576 cDNAs/ESTs (including positive and negative controls) were utilized on the current array platform. Arrays were prehybridized (6 hours) and hybridized (16 hours) in a solution consisting of 6X SSPE, 5X Denhardt's solution, 50% formamide, 0.1% sodium dodecyl sulfate (SDS), and denatured salmon sperm DNA (200 μg/ml) at 42°C in a rotisserie oven. Following hybridization, arrays were washed sequentially in2X standard saline citrate (SSC)/0.1% SDS, 1X SSC/0.1% SDS, and 0.5X SSC/0.1% SDS for 20 minutes each at 42°C. Arrays were exposed to a phosphor screen for 24 hours and developed on a phospho imager (GE-Healthcare). Hybridization signal intensity was quantified by subtracting background using empty vector (pBS Bluescript; Stratagene, La Jolla, CA). Expression of TC amplified RNA bound to each linearized cDNA was expressed as a ratio of the total hybridization signal intensity of the array (a global normalization approach). Global normalization effectively minimizes variation due to differences in the specific activity of the synthesized TC probe as well as the absolute quantity of probe present [40,41]. Data analysis generated an expression profile of relative changes in mRNA levels among NCI, AD/GAL−, and AD/GAL+ cholinergic NB neurons.

Quantitative PCR

Fifty and 100 neuron pools of AD/GAL− and AD/GAL+ cholinergic NB neurons were collected by microaspiration as above and used as sources of input RNA for quantitative PCR (qPCR) assays on a real-time PCR cycler (7900HT, Applied Biosystems). Human TaqMan hydrolysis probes designed against choline acetyltransferase (ChAT, the synthetic enzyme for acetylcholine; Taqman primer set identification #hs00758150) and glyceraldehyde-3 phosphate dehy-drogenase (GAPDH; #hs02758991) were utilized (Applied Biosystems) as described previously [38,42]. Standard curves and Ct values were measured using serial dilution standards obtained from total human brain RNA. The ddCT method was employed to

determine relative gene level differences with GAPDH qPCR products used as a control [42, 43].

Statistical analysis

Demographic variables (Table 1) were compared between the NCI and AD groups by the Mann-Whitney test. Expression levels of mRNAs were clustered and displayed using a bioinformatics and graphics software package (GeneLinker Gold, Predictive Patterns, Kingston, ON) [28–30]. Relative changes in hybridization signal intensity of individual transcripts in NCI, AD/GAL−, and AD/GAL+ cells were analyzed by oneway analysis of variance (ANOVA) with *post hoc* Newman-Keuls analysis. Level of significance was set at $p < 0.01$.

RESULTS AND DISCUSSION

Identification and accession of NCI, AD/GAL−, and AD/GAL+ cholinergic NB neurons

Dual immunohistochemistry revealed GAL-positive fibers (dark blue-black) in close association with $p75^{NTR}$ -ir cholinergic neurons (brown) within the anterior NB in both NCI and AD cases (Fig. 1). A semiquantitative scoring method (score = 1–3) was used to define NCI, AD/GAL−, and AD/GAL+ NB neurons for analysis (see Methods) [28,32,35]. In NCI cases, a fine network of GAL-ir fibers was seen coursing through the NB. Typically, there was either no visible evidence of GAL innervation of NB neurons or very sparse fiber apposition onto these cells (Fig. 1A). Both of these types of neurons were scored with a 1 (little or no innervation). In AD cases, the GAL fiber plexus was considerably denser (Fig. 1B–D). However, the majority of cells observed were either lightly (as in Fig. 1A, score = 1) or moderately (Fig. 1B, score = 2) innervated by fine GAL fibers. By contrast, GAL-hyperinnervated NB neurons were identified based on their dense innervation by thickened GAL fibers (Fig. 1C, D, score = 3). To maximize the likelihood of observing significant differences in gene expression between GAL-hyperinnervated and non-hyperinnervated cholinergic neurons, we accessed only NCI cells with a score = 1, AD/GAL− cells with a score = 1, and AD/GAL+ cells with a score = 3 from the anterior NB [28,32]. Accession of select NB neurons was achieved by aspiration with a micropipette under control of a vacuum source (Fig. 1, E–G).

Effects of GAL hyperinnervation on glutamate receptor mRNAs in NB neurons in AD

Custom cDNA array analysis of NCI, AD/GAL−, and AD/GAL+ NB neurons revealed a dynamic range of hybridization signal intensities for mRNAs encoding neurotransmitter receptors (Fig. 2A, B). Notably, whereas mRNA levels of the α-amino-3-hydroxy-5-methylisoxazole-4- propionic acid (AMPA) glutamate receptor (GluR) subunit GluR1 (Unigene/NCBI notation GRIA1) were reduced ~40% in both AD cell types compared to NCI cells, GluR2 (GRIA2) transcripts were significantly down-regulated ~65% only in AD/GAL − cells (Fig. 2B). The preservation of GluR2 levels in AD/GAL+ cells is intriguing given that AM-PA GluRs containing this subunit are considered calcium (Ca^{2+})-impermeable and that the loss of GluR2 expression is causally related with ischemic cell death associated with high intracellular Ca^{2+} levels [44,45]. Hence, the preservation of GluR2 levels in AD/GAL+ cells may render them less vulnerable than AD/GAL−neurons to Ca^{2+}-mediated excitotoxicity.

Effects of GAL hyperinnervation on calcium-related mRNAs in NB neurons in AD

The putative effects of GAL on NB neuronal membrane Ca^{2+} permeability through the maintenance of GluR2 transcript levels led us to explore the effects of GAL on other Ca^{2+}-mediated pathways (Fig. 3). In particular, mRNA levels of various members of the calpain family of Ca^{2+}-regulated cysteine proteases were differentially affected by GAL hyperinnerva-

tion of cholinergic NB neurons in AD. For instance, both calpain 1 (CAPN1 or μ-calpain) and calpain 2 (CAPN2 or μ-calpain) catalytic subunit mRNAs were increased ~80% in AD/GAL − cells compared to NCI cells. However, calpain 1 but not calpain 2 mRNA levels were reduced ~65% in AD/GAL+ cells compared to AD/GAL− cells (Fig. 3). Likewise, mRNA levels of the small regulatory calpain subunit (CAPNS1) were significantly increased ~70% only in AD/GAL− cells compared to NCI cells. In contrast, mRNA levels of the endogenous calpain inhibitor, calpistatin (CAST, Fig. 3) were unchanged in CBF neurons between NCI and AD (Fig. 3). These results indicate a relative lack of calpain system activation in AD/GAL+ relative to AD/GAL− cells. Significantly, calpain activation is widespread in the AD brain and has been implicated as a key mediator of Ca^{2+}-induced cellular degeneration by catalyzing the cleavage of structural and regulatory proteins [46,47].

We also analyzed genes encoding calbindin (CALB1), calretinin (CALB2), and parvalbumin (PVALB), three cytosolic proteins that bind Ca^{2+} with high affinity and play an important neuroprotective role in buffering intracellular Ca^{2+} levels [48,49]. mRNA levels of CALB1 and CALB2 were reduced ~40–50% in both types of AD NB neurons relative to NCI (Fig. 3), reminiscent of a previous report showing a loss of CALB1 protein immunoreactivity in these cells in AD cases [50]. These molecular alterations may signal an increased vulnerability of cholinergic NB neurons to Ca^{2+}-mediated neurotoxicity in AD [48,50]. PVALB transcripts were not detected in the cholinergic NB neurons examined (Fig. 3), consistent with their localization to non-cholinergic interneurons within the NB [51]. Finally, an analysis of genes encoding sub-units which give rise to P/Q-type (CACNA1A), N-type (CACNA1B), and L-type (CACNA1C) voltage-gated Ca^{2+} channels revealed that CACNA1B transcripts were increased 40% in AD/GAL− cells only compared to NCI (Fig. 3). As the predominant Ca^{2+} currentinthe neuronal somatodendritic compartment appears to be N-type [52], the upregulationof CACNA1B transcripts in AD/GAL− cells may result in increased intracellular Ca^{2+} flux in these cells in response to excitatory input, posing a potential source for supraphysiological cytosolic Ca^{2+} levels that may be absent in AD/GAL+ cells. Intriguingly, studies have shown that amyloid-β-induced toxicity in cultured primary neurons involve increased Ca^{2+} influx via the selective upregulation [53] and activation [54] of N-type channels. Hence, mi-croarray analysis of different Ca^{2+}-mediated pathways indicate that GAL hyperinnervation may exert neuroprotective effects on cholinergic NB neurons in AD by maintaining intracellular Ca^{2+} homeostasis.

Effects of GAL hyperinnervation on other functional classes of mRNAs

Relative hybridization signal intensities for several functional classes of genes on the custom-designed cD-NA arrays were also queried for differences among the three cell types examined (Fig. 4). GAL had no effect on the down-regulation of mRNAs encoding select synaptic membrane proteins, including presynaptic synaptophysin (SYP) [30] and postsynaptic drebrin (DBN1), or the cholinotrophic receptor tyrosine kinases TrkA (NTRK1) and TrkB (NTRK2) [55] in AD. Likewise, GAL had no effect on the AD-specific upregulation of estrogen receptor β mRNA (ESR2, Fig. 4). Notably, previous immunohistochemical studies have demonstrated both a decrease in the number of NB neurons immunopositive for TrkA [56] and an increase in the number of NB neurons immunopositive for estrogen receptor β protein [57] in AD relative to aged controls. With respect to mRNAs encoding apoptotic regulators, including bcl2, bax, and bad (Fig. 4) as well as members of the caspase family of pro-apoptotic proteases (not shown), there were no measurable differences in expression among NCI, AD/GAL−, and AD/GAL+ NB neurons.

In contrast, an analysis of mRNAs encoding antioxi-dant enzymes revealed that manganese superoxide dismutase 2 (SOD2) levels were similar in AD/GAL+ and NCI cells compared to the relative down-regulation of this transcript in AD/GAL− cells (Fig. 4). SOD2 protein

products are targeted to mitochondria where their activity is critical for detoxifying superoxide free radicals [58,59]. Given the data linking increased mitochondrial oxidative stress and reduced mitochondrial function in AD [60,61], the preservation of SOD2 gene expression in AD/GAL+ cells suggests that GAL may exert neuroprotective effects upon CBF neurons through the modulation of select antioxidant genes.

Among the mRNAs encoding enzymes involved in the ubiquitin-proteasome system, there was a selective reduction in levels of the deubiquitinating enzyme ubiquitin-specific protease 8 (USP8) in AD/GAL− cells that was not evident in AD/GAL+ cells (Fig. 4). Post-translational modification of proteins by ubiquitination regulates a wide range of cellular functions including protein stability and intracellular transport and evidence for defective ubiquitin-proteasome function is documented in the AD brain [62–64]. While the specific roles of the USP family of gene products in cell function are poorly understood, USP8 null mice exhibit embryonic lethality [65]. Moreover, cultured fibroblasts and liver tissue from USP8 null mice display an accu-mulationofubiquitinated proteins that colocalized with enlarged endosomes [65]. While it is unclear whether USP8 functions in a similar manner in cholinergic NB neurons, the data from peripheral tissue studies suggest that endosomal trafficking may be more efficient in AD/GAL+ than in AD/GAL− cells.

Finally, based on our observation that transcripts encoding two of the three phosphofructokinase glycolytic isozymes [PFKL (isozyme B, liver type) and PFKP (isozyme C, platelet type)] are upregulated in AD cells compared to NCI (Fig. 4), we further explored transcripts involved in glucose metabolism. In particular, mRNA levels of the glucose transporter GLUT2 (SLC2A2) were decreased in AD/GAL− cells but not in AD/GAL+ cells. GLUT2 protein is localized predominantly to neuronal dendrites in the mammalian brain [66] and *in vivo* cerebral blockade of GLUT2 induces aberrant insulin pathway signaling and spatial memory deficits in aged rats [67]. As such, reduced GLUT2 activity may contribute to the impairment in brain insulin signaling and glucose uptake observed in sporadic AD [68]. The preservation of GLUT2 mR-NA in GAL-hyperinnervated NB neurons in AD may indicate relatively normal glucose metabolism in these cells relative to non-hyperinnervated NB neurons.

Lack of GAL receptor mRNA regulation in cholinergic NB neurons in late stage AD

We previously reported that cholinergic NB neurons express all three GAL receptor (GALR1, GALR2, and GALR3) transcripts [28]. There was no difference in the expression level of any of these GALR transcripts in NCI, AD/GAL−, or AD/GAL+ cells (Fig. 2). It is interesting to note that we detected a trend toward a significant increase in levels of the GALR2 mRNA in NB neurons from AD relative to NCI cases ($p < 0.046$). This receptor subtype has been shown to elicit neuroprotective responses in rodent preparations challenged with amyloid-β [69], glutamate [70], or status epilepticus [71]. All the same, the lack of regulation of GALR expression in GAL-hyperinnervated neurons is reminiscent of our previous report that GALR2 and GALR3 subtype mRNA levels are unchanged in multiple brain regions of transgenic mice overexpressing GAL [72]. Moreover, these results indicate that the increased GAL binding seen within the CBF in late stage AD [18] is not likely linked to gene expression. Rather, this GALR plasticity response may be due to increased GALR protein stability or membrane recruitment or an increase in presynaptic GALRs on innervating fibers. Alternatively, it is possible that GALRs are also expressed by glial cells which may modulate the effects of GAL on CBF neuron gene expression.

Corroborative qPCR studies

We have previously demonstrated the sensitivity of the custom-designed cDNA array platform for detecting significant changes in cholinergic NB neuronal gene expression by corroborating

our array findings with qPCR using frozen CBF tissue from the same cases [55,73]. In the present study, we were unable to use frozen CBF tissue for qPCR since the AD/GAL− and AD/GAL+ cells are both present in the samples, thus precluding differentiation of specific gene expression profiles between the two cellular phenotypes. To surmount this problem, we microaspirated AD/GAL− and AD/GAL+ cells from tissue sections of the same cases and attempted to perform qPCR on the pooled cell samples (n = 50 or 100 neurons). Since we have previously shown that ChAT mRNA expression is upregu-lated in single AD/GAL+ compared to AD/GAL− neurons [35], we selected this cholinergic marker for feasibility qPCR validation experiments. Unfortunately, we were unable to detect reliable expression of ChAT levels in the pooled samples. Moreover, the expression levels of the housekeeping gene GAPDH were at the limit of detection, suggesting the sensitivity of current qPCR technology is too low for this type of analysis in human postmortem brain tissue subjected to double label immunohistochemistry for the identification of a select population of neurons. However, our previous qPCR studies support the validity of custom-designed microarray assessment of changes in gene expression in single cholinergic AD/GAL− and AD/GAL+ neurons [43,55, 73].

Functionality of GAL hyperinnervation of CBF neurons in AD

The functional consequence of GAL fiber plasticity within the NB of AD subjects has been controversial. For instance, GAL inhibits acetylcholine release from cholinergic terminals in rodent hippocampal preparations and disrupts cognitive performance in animals [3,5,74], suggesting that GAL overexpression may exacerbate the cholinergic deficit seen in late stage AD. On the other hand, GAL was found to elicit excitatory actions in cultured rodent cholinergic neurons [4] and to protect these cells from amyloid-β toxicity [69], raising the possibility that GAL upregulation promotes cholinergic tone and/or neuronal survival in the AD brain. The present molecular profiling study provides substantive evidence that GAL sustains the expression of genes subserving multiple neuroprotective mechanisms (e.g., calcium homeostasis, antioxidant expression, glucose transport) in hyperinnervated cholinergic NB neurons compared to non-hyperinnervatedneurons. These data are complementedby our previous expression profiling studies showing that AD/GAL+ NB neurons display increased levels of ChAT compared to NCI and AD/GAL− neurons [35] and that GAL hyperinnervation prevents the decreased production of protein phosphatase1subtype mRNAs (PP1a and PP1g) in AD/GAL− cells [75], potentially attenuating phosphorylation events involved in neurofibrillary tangle formation [76]. It is important to note that GAL has not yet been shown to regulate the expression of these gene classes in neuronal cell culture models under naïve or neurotoxic conditions. Nonetheless, when the effects of GAL are indexed by single cell gene expression in postmortem tissue, it appears that this neuropeptide exerts a neuroprotective effect upon CBF neurons in AD. In support of this hypothesis, GAL hyperinnervation and GAL binding sites in AD are greatest in the anterior subfields of the NB where the least amount of cholinergic neuronal degeneration occurs, whereas GAL over-expression is sparse in the posterior subfields of the NB where degeneration is greatest [15, 18,77,78].

These data suggest a beneficial role for GAL in AD contrary to the well-established observation that GAL can inhibit rodent cholinergic transmission [3,5]. Hok-felt has recently suggested that GAL may have opposing effects on cholinergic projection neurons depending on the site of innervation, inhibiting acetylcholine transmission in the axonal compartment, and stimulating cholinergic function in the somatodendritic compartment [79]. Alternatively, GAL may have species-specific effects on CBF neurons [19]. Given the diverse repertoire of context-dependent GALR signaling pathways (e.g., GALR1 inhibits adenylyl cyclase or activates extracellular-regulated kinase, GALR2 activates phospholipase C or inhibits adenylyl cyclase [80,81]), delineating the GALR(s) activated by GAL in the human NB will be critical for

clarifying the functional effects of GAL in AD. Our observations that cholinergic NB perikarya express all three GALR transcripts but exhibitno alterations in these transcripts upon GAL hyperinnervation do not offer any additional clues to the predominant GALR pathways activated in AD/GAL+ cells. Resolution of this issue is complicated by the lack of GALR subtype-specific antibodies and the slow development of GALR subtype-specific ligands [75]. Nevertheless, the present findings provide a rationale for the continued explorationof GAL as a potential tool for the pharmacotherapeutic augmentation of basocortical cholinergic neuron function during the progression of AD.

Acknowledgments

We thank M. Nadeem and S. Dar for expert technical assistance. This work was supported by the National Institutes of Health (AG14449, AG16088, AG09466 AG10161, AG17617, NS48447, and AG26032) and the Illinois Department of Public Health.

Authors' disclosures available online (http://www.j-alz.com/disclosures/view.php?id=79).

REFERENCES

1. Crawley JN. Galanin-acetylcholine interactions: relevance to memory and Alzheimer's disease. Life Sci 1996;58:2185–2199. [PubMed: 8649205]
2. Dutar P, Lamour Y, Nicoll RA. Galanin blocks the slow cholinergic EPSPin CA1 pyramidal neurons from ventral hippocampus. Eur J Pharmacol 1989;164:355–360. [PubMed: 2474449]
3. Fisone G, Wu CF, Consolo S, Nordstrom O, Brynne N, Bartfai T, Melander T, Hokfelt T. Galanin inhibits acetylcholine release in the ventral hippocampus of the rat: histochemical, autoradiographic, *in vivo*, and *in vitro* studies. Proc Natl Acad Sci USA 1987;84:7339–7343. [PubMed: 2444980]
4. Jhamandas JH, Harris KH, MacTavish D, Jassar BS. Novel excitatory actions of galanin on rat cholinergic basal forebrain neurons: implications for its role in Alzheimer's disease. J Neurophysiol 2002;87:696–704. [PubMed: 11826038]
5. Ogren SO, Kehr J, Schott PA. Effects of ventral hippocampal galanin on spatial learning and on *in vivo* acetylcholine release in the rat. Neuroscience 1996;75:1127–1140. [PubMed: 8938746]
6. Mesulam MM, Mufson EJ, Levey AI, Wainer BH. Cholinergic innervation of cortex by the basal forebrain: cytochemistry and cortical connections of the septal area, diagonal band nuclei, nucleus basalis (substantia innominata), and hypothalamus in the rhesus monkey. J Comp Neurol 1983;214:170–197. [PubMed: 6841683]
7. Bartus RT. On neurodegenerative diseases, models, and treatment strategies: lessons learned and lessons forgotten a generation following the cholinergic hypothesis. Exp Neurol 2000;163:495–529. [PubMed: 10833325]
8. Baxter MG, Chiba AA. Cognitive functions of the basal forebrain. Curr Opin Neurobiol 1999;9:178–183. [PubMed: 10322180]
9. Sarter M, Bruno JP, Turchi J. Basal forebrain afferent projections modulating cortical acetylcholine, attention, and implications for neuropsychiatric disorders. Ann N Y Acad Sci 1999;877:368–382. [PubMed: 10415659]
10. Davies P, Maloney AJ. Selective loss of central cholinergic neurons in Alzheimer's disease. Lancet 1976;2:1403. [PubMed: 63862]
11. Whitehouse PJ, Price DL, Clark AW, Coyle JT, DeLong MR. Alzheimer disease: evidence for selective loss of cholinergic neurons in the nucleus basalis. Ann Neurol 1981;10:122–126. [PubMed: 7283399]
12. DeKosky ST, Harbaugh RE, Schmitt FA, Bakay RA, Chui HC, Knopman DS, Reeder TM, Shetter AG, Senter HJ, Markesbery WR. Cortical biopsy in Alzheimer's disease: diagnostic accuracy and neurochemical, neuropathological, and cognitive correlations. Intraventricular Bethanecol Study Group. Ann Neurol 1992;32:625–632. [PubMed: 1360195]
13. Wilcock GK, Esiri MM, Bowen DM, Smith CC. Alzheimer's disease. Correlation of cortical choline acetyltransferase activity with the severity of dementia and histolog-ical abnormalities. J Neurol Sci 1982;57:407–417. [PubMed: 7161627]

14. Bowser R, Kordower JH, Mufson EJ. A confocal microscopic analysis of galaninergic hyperinnervation of cholinergic basal forebrain neurons in Alzheimer's disease. Brain Pathol 1997;7:723–730. [PubMed: 9161723]
15. Chan-Palay V. Galanin hyperinnervates surviving neurons of the human basal nucleus of Meynert in dementias of Alzheimer's and Parkinson's disease: a hypothesis for the role of galanin in accentuating cholinergic dysfunction in dementia. J Comp Neurol 1988;273:543–557. [PubMed: 2463283]
16. Mufson EJ, Cochran E, Benzing W, Kordower JH. Galaninergic innervation of the cholinergic vertical limb of the diagonal band (Ch2) and bed nucleus of the stria terminalis in aging, Alzheimer's disease and Down's syndrome. Dementia 1993;4:237–250. [PubMed: 7505157]
17. Beal MF, MacGarvey U, Swartz KJ. Galanin immunoreactivity is increased in the nucleus basalis of Meynert in Alzheimer's disease. Ann Neurol 1990;28:157–161. [PubMed: 1699471]
18. Mufson EJ, Deecher DC, Basile M, Izenwasse S, Mash DC. Galanin receptor plasticity within the nucleus basalis in early and late Alzheimer's disease: an *in vitro* autoradiographic analysis. Neuropharmacology 2000;39:1404–1412. [PubMed: 10818256]
19. Counts SE, Perez SE, Mufson EJ. Galanin – 25 years with a multitalented neuropeptide: Galanin in Alzheimer's disease: Neuroinhibitory or neuroprotective? Cell Mol Life Sci 2008;65:1842–1853. [PubMed: 18500641]
20. Bennett DA, Wilson RS, Schneider JA, Evans DA, Beckett LA, Aggarwal NT, Barnes LL, Fox JH, Bach J. Natural history of mild cognitive impairment in older persons. Neurology 2002;59:198–205. [PubMed: 12136057]
21. Counts SE, Nadeem M, Wuu J, Ginsberg SD, Saragovi HU, Mufson EJ. Reduction of cortical TrkA but not p75(NTR) protein in early-stage Alzheimer's disease. Ann Neurol 2004;56:520–531. [PubMed: 15455399]
22. DeKosky ST, Ikonomovic MD, Styren SD, Beckett L, Wisniewski S, Bennett DA, Cochran EJ, Kordower JH, Mufson EJ. Upregulation of choline acetyltransferase activity in hippocampus and frontal cortex of elderly subjects with mild cognitive impairment. Ann Neurol 2002;51:145–155. [PubMed: 11835370]
23. Mufson EJ, Ma SY, Dills J, Cochran EJ, Leurgans S, Wuu J, Bennett DA, Jaffar S, Gilmor ML, Levey AI, Kordower JH. Loss of basal forebrain P75(NTR) immunoreactivity in subjects with mild cognitive impairment and Alzheimer's disease. J Comp Neurol 2002;443:136–153. [PubMed: 11793352]
24. McKhann G, Drachman D, Folstein M, Katzman R, Price D, Stadlan EM. Clinical diagnosis of Alzheimer's disease: report of the NINCDS-ADRDA Work Group under the auspices of Department of Health and Human Services Task Force on Alzheimer's Disease. Neurology 1984;34:939–944. [PubMed: 6610841]
25. Folstein MF, Folstein SE, McHugh PR. Mini-mental state. A practical method for grading the cognitive state of patients for the clinician. J Psychiatr Res 1975;12:189–198. [PubMed: 1202204]
26. Bennett DA, Schneider JA, Bienias JL, Evans DA, Wilson RS. Mild cognitive impairment is related to Alzheimer disease pathology and cerebral infarctions. Neurology 2005;64:834–841. [PubMed: 15753419]
27. Mirra SS, Heyman A, McKeel D, Sumi SM, Crain BJ, Brownlee LM, Vogel FS, Hughes JP, van Belle G, Berg L. The Consortium to Establish a Registry for Alzheimer's Disease (CERAD). Part II. Standardization of the neuropathologic assessment of Alzheimer's disease. Neurology 1991;41:479–486. [PubMed: 2011243]
28. Counts SE, Chen EY, Che S, Ikonomovic MD, Wuu J, Ginsberg SD, Dekosky ST, Mufson EJ. Galanin fiber hypertrophy within the cholinergic nucleus basalis during the progression of Alzheimer's disease. Dement Geriatr Cogn Disord 2006;21:205–214. [PubMed: 16410678]
29. Ginsberg SD, Che S, Counts SE, Mufson EJ. Shift in the ratio of three-repeat tau and four-repeat tau mRNAs in individual cholinergic basal forebrain neurons in mild cognitive impairment and Alzheimer's disease. J Neurochem 2006;96:1401–1408. [PubMed: 16478530]
30. Mufson EJ, Counts SE, Ginsberg SD. Gene expression profiles of cholinergic nucleus basalis neurons in Alzheimer's disease. Neurochem Res 2002;27:1035–1048. [PubMed: 12462403]

31. Ginsberg SD, Crino PB, Lee VM, Eberwine JH, Trojanowski JQ. Sequestration of RNA in Alzheimer's disease neu-rofibrillary tangles and senile plaques. Ann Neurol 1997;41:200–209. [PubMed: 9029069]
32. Sendera TJ, Ma SY, Jaffar S, Kozlowski PB, Kordower JH, Mawal Y, Saragovi HU, Mufson EJ. Reduction in TrkA-immunoreactive neurons is not associated with an overexpres-sionof galaninergic fibers within the nucleus basalisin Down's syndrome. J Neurochem 2000;74:1185–1196. [PubMed: 10693951]
33. Mufson EJ, Bothwell M, Hersh LB, Kordower JH. Nerve growth factor receptor immunoreactive profiles in the normal, aged human basal forebrain: colocalization with cholinergic neurons. J Comp Neurol 1989;285:196–217. [PubMed: 2547849]
34. Schatteman GC, Gibbs L, Lanahan AA, Claude P, Bothwell M. Expression of NGF receptor in the developing and adult primate central nervous system. J Neurosci 1988;8:860–873. [PubMed: 2831315]
35. Counts SE, He B, Che S, Ginsberg SD, Mufson EJ. Galanin hyperinnervation upregulates choline acetyltrans-ferase expression in cholinergic basal forebrain neurons in Alzheimer's disease. Neurodegener Dis 2008;5:228–231. [PubMed: 18322398]
36. Che S, Ginsberg SD. Amplification of RNA transcripts using terminal continuation. Lab Invest 2004;84:131–137. [PubMed: 14647400]
37. Ginsberg SD, Che S. Combined histochemical staining, RNA amplification, regional, and single cell cDNA analysis within the hippocampus. Lab Invest 2004;84:952–962. [PubMed: 15107803]
38. Alldred MJ, Che S, Ginsberg SD. Terminal continuation (TC) RNA amplification enables expression profiling using minute RNA input obtained from mouse brain. Int J Mol Sci 2008;9:2091–2104. [PubMed: 19165351]
39. Ginsberg SD, Che S. RNA amplificationin brain tissues. Neurochem Res 2002;27:981–992. [PubMed: 12462399]
40. Ginsberg SD, Elarova I, Ruben M, Tan F, Counts SE, Eberwine JH, Trojanowski JQ, Hemby SE, Mufson EJ, Che S. Single-cell gene expression analysis: implications for neurodegenerative and neuropsychiatric disorders. Neurochem Res 2004;29:1053–1064. [PubMed: 15176463]
41. Hemby SE, Ginsberg SD, Brunk B, Arnold SE, Trojanowski JQ, Eberwine JH. Gene expression profile for schizophrenia: discrete neuron transcription patterns in the entorhinal cortex. Arch Gen Psychiatry 2002;59:631–640. [PubMed: 12090816]
42. Ginsberg SD. Transcriptional profiling of small samples in the central nervous system. Methods Mol Biol 2008;439:147–158. [PubMed: 18370101]
43. Ginsberg SD, Mirnics K. Functional genomic methodologies. Prog Brain Res 2006;158:15–40. [PubMed: 17027690]
44. Liu S, Lau L, Wei J, Zhu D, Zou S, Sun HS, Fu Y, Liu F, Lu Y. Expression of Ca(2+)-permeable AMPA receptor channels primes cell death in transient forebrain ischemia. Neuron 2004;43:43–55. [PubMed: 15233916]
45. Oguro K, Oguro N, Kojima T, Grooms SY, Calderone A, Zheng X, Bennett MV, Zukin RS. Knockdown of AMPA receptor GluR2 expression causes delayed neurodegeneration and increases damage by sublethal ischemia in hippocampal CA1 and CA3 neurons. J Neurosci 1999;19:9218–9227. [PubMed: 10531425]
46. Nixon RA, Saito KI, Grynspan F, Griffin WR, Katayama S, Honda T, Mohan PS, Shea TB, Beermann M. Calcium-activated neutral proteinase (calpain) system in aging and Alzheimer's disease. Ann N Y Acad Sci 1994;747:77–91. [PubMed: 7847693]
47. Rao MV, Mohan PS, Peterhoff CM, Yang DS, Schmidt SD, Stavrides PH, Campbell J, Chen Y, Jiang Y, Paskevich PA, Cataldo AM, Haroutunian V, Nixon RA. Marked calpastatin (CAST) depletion in Alzheimer's disease accelerates cytoskeleton disruption and neurodegeneration: neuroprotection by CAST overexpression. J Neurosci 2008;28:12241–12254. [PubMed: 19020018]
48. Mattson MP, Rychlik B, Chu C, Christakos S. Evidence for calcium-reducing and excito-protective roles for the calcium-binding protein calbindin-D28k in cultured hippocampal neurons. Neuron 1991;6:41–51. [PubMed: 1670921]
49. Miller RJ. The control of neuronal Ca2+ homeostasis. Prog Neurobiol 1991;37:255–285. [PubMed: 1947178]

50. Geula C, Bu J, Nagykery N, Scinto LF, Chan J, Joseph J, Parker R, Wu CK. Loss of calbindin-D28k from aging human cholinergic basal forebrain: relation to neuronal loss. J Comp Neurol 2003;455:249–259. [PubMed: 12454989]
51. Brauer K, Schober A, Wolff JR, Winkelmann E, Luppa H, Luth HJ, Bottcher H. Morphology of neurons in the rat basal forebrain nuclei: comparison between NADPH-diaphorase histochemistry and immunohistochemistry of glutamic acid decarboxylase, choline acetyltransferase, somatostatin and parvalbumin. J Hirnforsch 1991;32:1–17. [PubMed: 1687412]
52. Delmas P, Abogadie FC, Buckley NJ, Brown DA. Calcium channel gating and modulation by transmitters depend on cellular compartmentalization. Nat Neurosci 2000;3:670–678. [PubMed: 10862699]
53. Price SA, Held B, Pearson HA. Amyloid beta protein increases Ca2+ currents in rat cerebellar granule neurones. Neuroreport 1998;9:539–545. [PubMed: 9512403]
54. MacManus A, Ramsden M, Murray M, Henderson Z, Pearson HA, Campbell VA. Enhancement of (45)Ca(2+) influx and voltage-dependent Ca(2+) channel activity by beta-amyloid-(1–40) in rat cortical synaptosomes and cultured cortical neurons. Modulation by the proinflammatory cytokine interleukin-1beta. J Biol Chem 2000;275:4713–4718. [PubMed: 10671502]
55. Ginsberg SD, Che S, Wuu J, Counts SE, Mufson EJ. Down regulation oftrk but not p75NTR gene expression in single cholinergic basal forebrain neurons mark the progression of Alzheimer's disease. J Neurochem 2006;97:475–487. [PubMed: 16539663]
56. Mufson EJ, Ma SY, Cochran EJ, Bennett DA, Beckett LA, Jaffar S, Saragovi HU, Kordower JH. Loss of nucleus basalis neurons containing trkA immunoreactivity in individuals with mild cognitive impairment and early Alzheimer's disease. J Comp Neurol 2000;427:19–30. [PubMed: 11042589]
57. Ishunina TA, Swaab DF. Increased expression of estrogen receptor alpha and beta in the nucleus basalis of Meynert in Alzheimer's disease. Neurobiol Aging 2001;22:417–426. [PubMed: 11378248]
58. Balaban RS, Nemoto S, Finkel T. Mitochondria, oxidants, and aging. Cell 2005;120:483–495. [PubMed: 15734681]
59. Liang LP, Patel M. Mitochondrial oxidative stress and increased seizure susceptibility in Sod2(−/+) mice. Free Radic Biol Med 2004;36:542–554. [PubMed: 14980699]
60. Perry G, Castellani RJ, Hirai K, Smith MA. Reactive oxygen species mediate cellular damage in alzheimer disease. J Alzheimers Dis 1998;1:45–55. [PubMed: 12214011]
61. Wang J, Xiong S, Xie C, Markesbery WR, Lovell MA. Increased oxidative damage in nuclear and mitochondrial DNA in Alzheimer's disease. J Neurochem 2005;93:953–962. [PubMed: 15857398]
62. Choi J, Levey AI, Weintraub ST, Rees HD, Gearing M, Chin LS, Li L. Oxidative modifications and down-regulation of ubiquitin carboxyl-terminal hydrolase L1 associated with idiopathic Parkinson's and Alzheimer's diseases. J Biol Chem 2004;279:13256–13264. [PubMed: 14722078]
63. Keller JN, Hanni KB, Markesbery WR. Impaired proteasome function in Alzheimer's disease. J Neurochem 2000;75:436–439. [PubMed: 10854289]
64. Pasinetti GM. Use of cDNA microarray in the search for molecular markers involved in the onset of Alzheimer's disease dementia. J Neurosci Res 2001;65:471–476. [PubMed: 11550214]
65. Niendorf S, Oksche A, Kisser A, Lohler J, Prinz M, Schorle H, Feller S, Lewitzky M, Horak I, Knobeloch KP. Essential role of ubiquitin-specific protease 8 for receptor tyrosine kinase stability and endocytic trafficking *in vivo*. Mol Cell Biol 2007;27:5029–5039. [PubMed: 17452457]
66. Arluison M, Quignon M, Thorens B, Leloup C, Penicaud L. Immunocytochemical localization of the glucose transporter 2 (GLUT2) in the adult rat brain. II. Electron microscopic study. J Chem Neuroanat 2004;28:137–146. [PubMed: 15482900]
67. Salkovic-Petrisic M, Tribl F, Schmidt M, Hoyer S, Riederer P. Alzheimer-like changes in protein kinase B and glycogen synthase kinase-3 in rat frontal cortex and hippocampus after damage to the insulin signalling pathway. J Neurochem 2006;96:1005–1015. [PubMed: 16412093]
68. Hoyer S. Glucose metabolism and insulin receptor signal transduction in Alzheimer disease. Eur J Pharmacol 2004;490:115–125. [PubMed: 15094078]
69. Ding X, Mac Tavish D, Kar S, Jhamandas JH. Galanin attenuates beta-amyloid (Abeta) toxicity in rat cholinergic basal forebrain neurons. Neurobiol Dis 2006;21:413–420. [PubMed: 16246567]

70. Pirondi S, Fernandez M, Schmidt R, Hokfelt T, Giardino L, Calza L. The galanin-R2 agonist AR-M1896 reduces glutamate toxicity in primary neural hippocampal cells. J Neurochem 2005;95:821–833. [PubMed: 16248891]
71. Mazarati A, Lu X, Kilk K, Langel U, Wasterlain C, Bartfai T. Galanin type 2 receptors regulate neuronal survival, susceptibility to seizures and seizure-induced neurogenesis in the dentate gyrus. Eur J Neurosci 2004;19:3235–3244. [PubMed: 15217380]
72. He B, Counts SE, Perez SE, Hohmann JG, Koprich JB, Lipton JW, Steiner RA, Crawley JN, Mufson EJ. Ectopic galanin expression and normal galanin receptor 2 and galanin receptor 3 mRNA levels in the forebrain of galanin transgenic mice. Neuroscience 2005;133:371–380. [PubMed: 15885921]
73. Counts SE, He B, Che S, Ikonomovic MD, DeKosky ST, Ginsberg SD, Mufson EJ. Alpha7 nicotinic receptor up-regulation in cholinergic basal forebrain neurons in Alzheimer disease. Arch Neurol 2007;64:1771–1776. [PubMed: 18071042]
74. McDonald MP, Gleason TC, Robinson JK, Crawley JN. Galanin inhibits performance on rodent memory tasks. Ann N Y Acad Sci 1998;863:305–322. [PubMed: 9928180]
75. Counts SE, Perez SE, Ginsberg SD, De Lacalle S, Mufson EJ. Galanin in Alzheimer disease. Mol Interv 2003;3:137–156. [PubMed: 14993421]
76. Trojanowski JQ, Lee VM. Phosphorylation of paired helical filament tau in Alzheimer's disease neurofibrillary lesions: focusing on phosphatases. FASEB J 1995;9:1570–1576. [PubMed: 8529836]
77. Mufson EJ, Bothwell M, Kordower JH. Loss of nerve growth factor receptor-containing neurons in Alzheimer's disease: a quantitative analysis across subregions of the basal forebrain. Exp Neurol 1989;105:221–232. [PubMed: 2548888]
78. Vogels OJ, Broere CA, ter Laak HJ, ten Donkelaar HJ, Nieuwenhuys R, Schulte BP. Cell loss and shrinkage in the nucleus basalis Meynert complex in Alzheimer's disease. Neurobiol Aging 1990;11:3–13. [PubMed: 2183081]
79. Hokfelt T. Galanin and its receptors: Introduction to the Third International Symposium, San Diego, California, USA, 21–22 October 2004. Neuropeptides 2005;39:125–142. [PubMed: 15908000]
80. Smith KE, Forray C, Walker MW, Jones KA, Tamm JA, Bard J, Branchek TA, Linemeyer DL, Gerald C. Expression cloning of a rat hypothalamic galanin receptor coupled to phosphoinositide turnover. J Biol Chem 1997;272:24612–24616. [PubMed: 9305929]
81. Wang S, Hashemi T, Fried S, Clemmons AL, Hawes BE. Differential intracellular signaling of the GalR1 and GalR2 galanin receptor subtypes. Biochemistry 1998;37:6711–6717. [PubMed: 9578554]

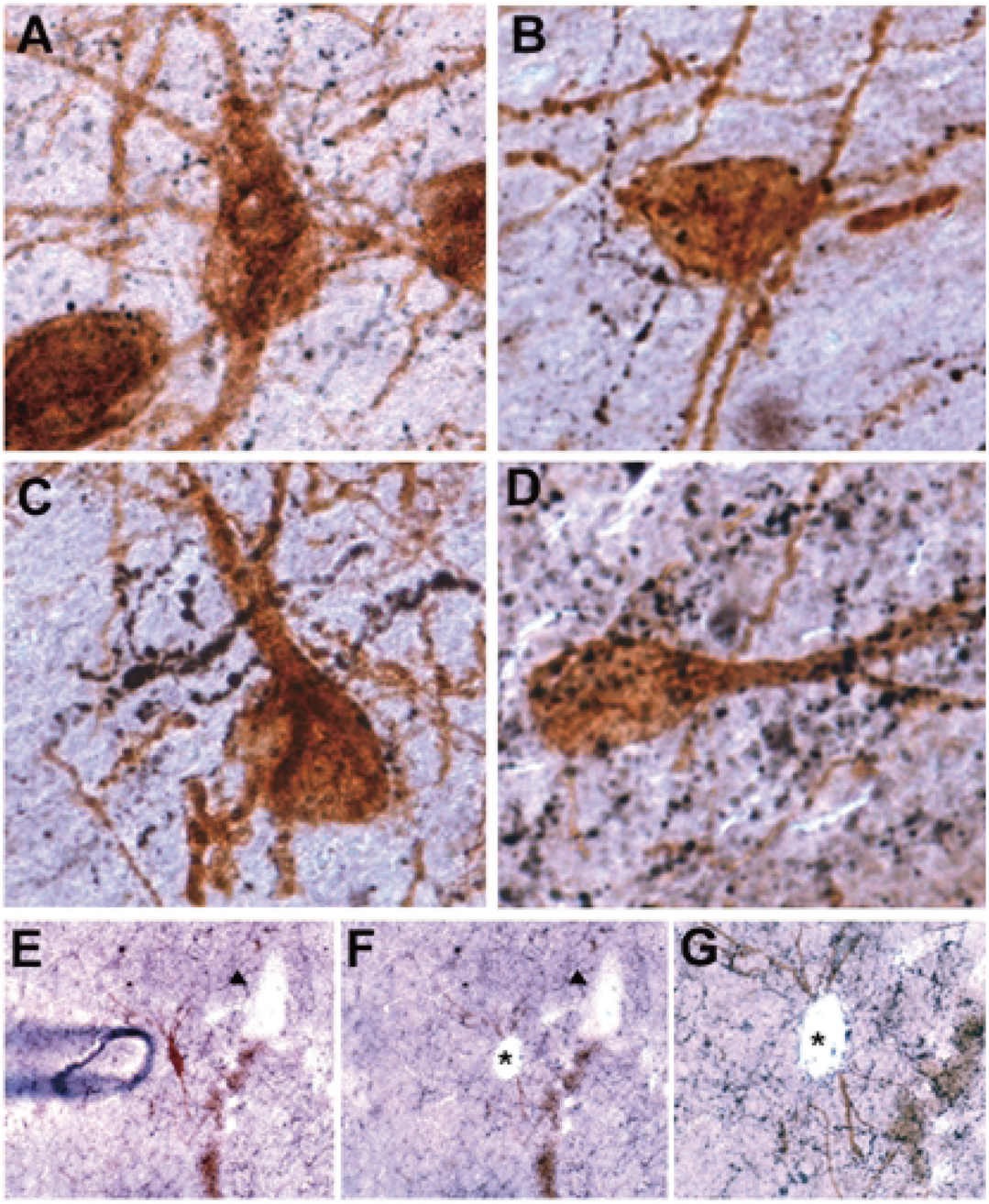

Fig. 1.

Identification of GAL hyperinnervated and non-hyperinnervated cholinergic NB neurons. (A) Photomicrograph shows a cholinergic NB neuron (*brown*) from a NCI case associated with very sparse, fine caliber GAL-immunoreactive fibers (*blue/black*). This neuron was scored with a 1 based on a semi-quantitative GAL innervation rating scale (see Methods). (B) Photomicrograph shows a cholinergic NB neuron from a late stage AD case lightly innervated with fine caliber GAL fibers which were relatively more abundant than the neurons shown in (A). This cell was scored with a 2. (C, D) Photomicrographs show cholinergic NB neurons from AD cases hyperinnervated with abundant thickened GAL-immunoreactive fibers. These neurons were scored with a 3. (E-G) Sequential series of photomicrographs showing isolation

(E) and accession (F) of a GAL-hyperinnervated NB neuron within the CBF of an AD subject. Photomicrograph in (G) is a magnification of (F). * denotes site of NB neuron microaspiration.

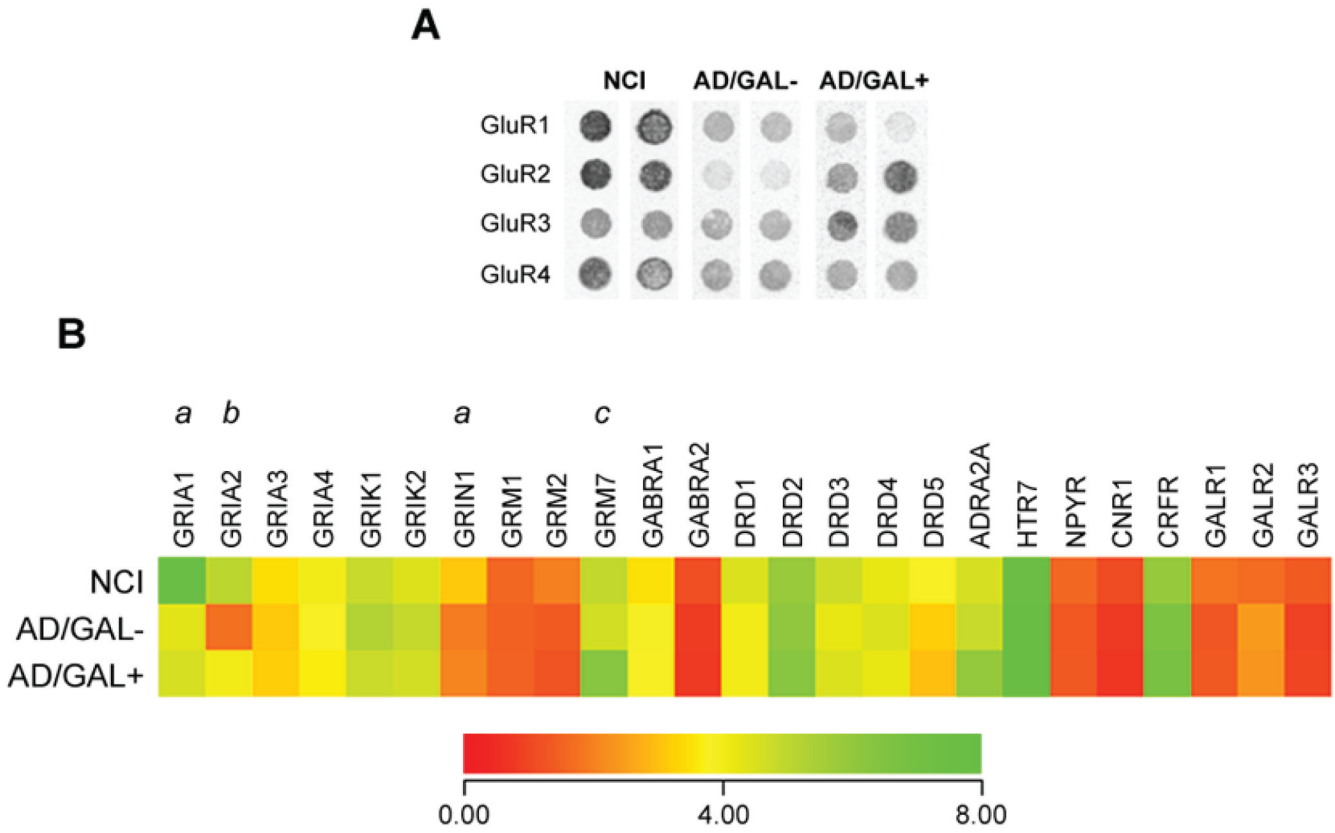

Fig. 2.

GAL hyperinnervated NB neurons display preserved GluR2 transcripts levels in AD. (A) Representative custom-designed microarray expression data showing relative hybridization signal intensities for GluR1, GluR2, GluR3, and GluR4 AMPAreceptor mRNAs in NCI, AD/GAL−, and AD/GAL+ cholinergic NB neurons. (B) Heatmap illustrating relative mRNA expression levels (red to green = increasing levels) of AMPA GluR subunits GluR1 (Unigene/NCBI notation GRIA1), GluR2 (GRIA2), GluR3 (GRIA3), and GluR4 (GRIA4), kainate GluR subunits GluR5 (GRIK1) and GluR6 (GRIK2), N-methyl D-aspartate (NMDA) GluR subunit NR1 (GRIN1), metabotropic GluRs mGluR1 (GRM1), mGluR2 (GRM2), and mGluR7 (GRM7), γ-aminobutyric acid (GABA) receptor subunits $GABA_A$ α-1 (GABRA1)and $GABA_A$ α-2(GABRA2), dopamine receptors D1-D5 (DRD1-5), α_{2A}-adrenergic receptor (ADRA2A), serotonin receptor 7 (HTR7), neuropeptide Y receptor (NPYR), CB1 cannabinoid receptor (CNR1), corticotrophin releasing factor receptor (CRFR), and GAL receptors 1–3 (GALR1-GALR3). *a* = NCI > AD/GAL−, AD/GAL+, $p < 0.01$; *b* = NCI, AD/GAL+ > AD/GAL−, $p < 0.01$; *c* = AD/GAL+ > NCI, AD/GAL−, $p < 0.01$.

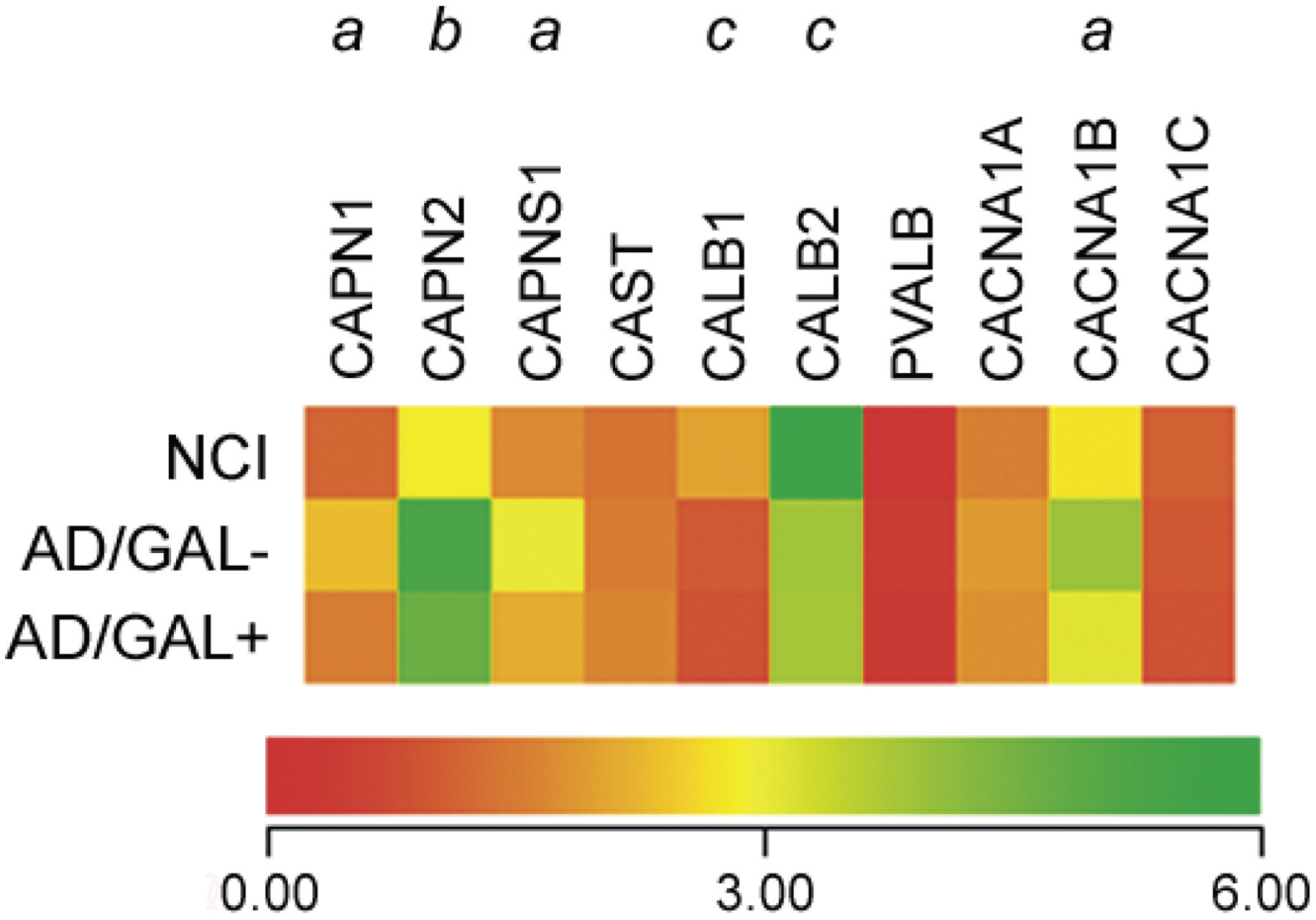

Fig. 3.

GAL hyperinnervated NB neurons display preserved calpain transcripts levels in AD. Heatmap illustrating relative mRNA expression levels (red to green = increasing levels) of the μ-calpain (Unigene/NCBI notation CAPN1) and μ-calpain (CAPN2) catalytic subunits, the small capain regulatory subunit (CAPNS1), calpistatin (CAST), calbindin (CALB1), calretinin (CALB2), parvalbumin (PVALB), and the P/Q-type (CACNA1A), N-type (CACNA1B), and L-type (CACNA1A) voltage-gated Ca^{2+} channel subunits. *a* = AD/GAL− > NCI, AD/GAL+, $p < 0.01$; *b* = AD/GAL−, AD, GAL+ > NCI, $p < 0.01$; *c* = NCI > AD/GAL−, AD/GAL+, $p < 0.01$.

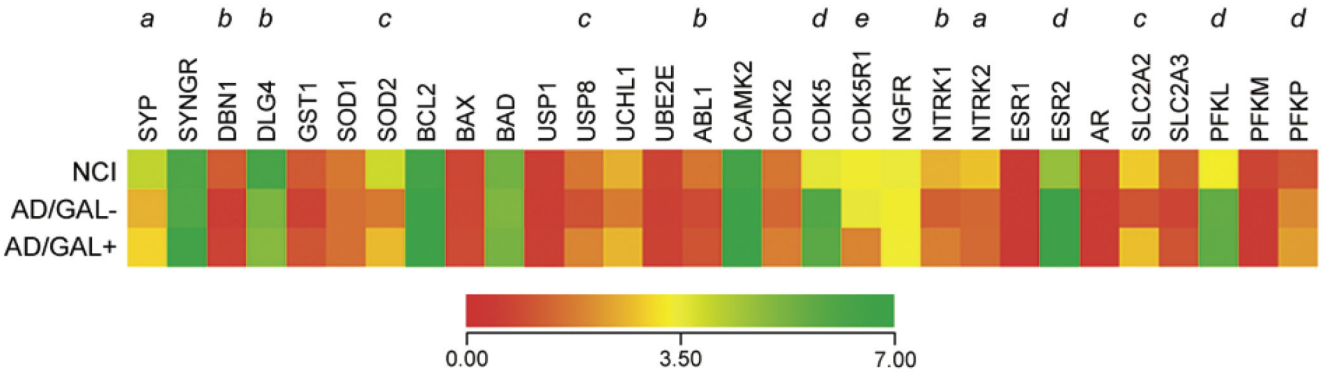

Fig. 4.

GAL hyperinnervated NB neurons display preserved antioxidant, deubiquitinating, and glucose transport transcripts in AD. Heatmap illustrating relative mRNA expression levels (red to green = increasing levels) of synaptophysin (Unigene/NCBI notation SYP), synaptogyrin (SYNGR), drebrin 1 (DRB1), postsynaptic density PSD95 (DLG4), glutathione-S-transferase 1 (GST1), superoxide dismutase 1 (SOD1), superoxide dismutase 2 (SOD2), bcl2 (BCL2), bax (BAX), bad (BAD), ubiquitin-specific protease 1 (USP1), ubiquitin-specific protease 8 (USP8), ubiquitin carboxyl-terminal esterase L1 (UCHL1), ubiquitin-conjugating enzyme E2E 1 (UBE2E), abl1 tyrosine kinase (ABL1), Ca^{2+}/calmodulin-dependent protein kinase II (CAMK2), cyclin-dependent kinase 2 (CDK2), cyclin-dependent kinase 5 (CDK5), p35 cdk5 regulatory subunit (CDK5R1), $p75^{NTR}$ neurotrophin receptor (NGFR), trkA (NTRK1), trkB (NTRK2), estrogen receptor α (ESR1), estrogen receptor β (ESR2), androgen receptor (AR), glucose transporters GLUT2 (SLC2A2) and GLUT3 (SLC2A3), and phosphofructokinase liver type (PFKL), muscle type (PFKM) and platelet type (PFKP) isozymes. *a* = NCI > AD/GAL−, AD/GAL+, $p < 0.001$; *b* = NCI > AD/GAL−, AD/GAL+, $p < 0.01$; *c* = NCI, AD/GAL + > AD/GAL−, $p < 0.01$; *d* = AD/GAL−, AD/GAL+ > NCI, $p < 0.01$; *e* = NCI, AD/GAL− > AD/GAL+, $p < 0.01$.

Table 1

Case demographics

	NCI	AD	*p* value*
n	6	6	
Age (mean ± SD) (range)	83.0 ± 5.2 (78–91)	79.1 ± 7.1 (73–92)	0.33
PMI (hours) (range)	5.7 ± 2.3 (3.5–9)	7.5 ± 5.4 (3–18)	0.79
MMSE (range)	27.8 ± 1.3 (26–29)	4.7 ± 3.5 (1–8)	0.01

*Mann-Whitney.